The Landscape of *Parkin* Variants Reveals Pathogenic Mechanisms and Therapeutic Targets in PD

Wei Yi[1], Emma J. MacDougall[1], Matthew Y. Tang[1], Andrea I. Krahn[1], Ziv Gan-Or[2], Jean-François Trempe[3], Edward A. Fon[1*]

[1]McGill Parkinson Program, Neurodegenerative Diseases Group, Department of Neurology and Neurosurgery, Montreal Neurological Institute, McGill University, Montreal, Quebec, Canada H3A 2B4. Phone: +1-514-398-8398.

[2]Montreal Neurological Institute and Hospital, Department of Neurology & Neurosurgery, Department of Human Genetics, McGill University, Montreal, Quebec, Canada H3A 1A1. Phone: +1-514-398-5845.

[3]Groupe de recherche axé sur la structure des protéines, Department of Pharmacology and Therapeutics, McGill University, Montreal, Quebec, Canada H3G 1Y6. Phone: +1-514-398-6833.

* Correspondence and requests for materials should be addressed to E.A.F. (email: ted.fon@mcgill.ca).

Conflict of interest: The authors have declared that no conflict of interest exists.

Abstract

Mutations in *Parkin* (*PARK2*) are the most common genetic cause of early-onset Parkinson's disease (PD). *Parkin* encodes an E3 ubiquitin ligase implicated in the turnover of damaged mitochondria. Hundreds of *Parkin* missense variants have been reported in public databases, yet the role of most of them in PD remains unclear. Here we analyzed *Parkin* variants using clinical, experimental, and structural modeling approaches. For most variants, clinical evidence alone was insufficient to determine pathogenicity. Utilizing a cell model that allows measurement of Parkin-mediated mitophagy and Parkin stability, 51 variants were classified into five groups based on their effect on Parkin function. Most variants were like wildtype and unexpectedly, several enhanced mitophagy. A minority destabilized Parkin or severely disrupted Parkin-mediated mitophagy, most of which were also determined as *pathogenic* based on clinical evidence alone. Structural simulation predicted multiple mechanisms for both the increase and decrease in Parkin function. Interestingly, impaired mitophagy in several of the most common *pathogenic* Parkin variants could be rescued both by naturally-occurring (p.V224A) and structure-guided designer (p.W403A; p.F146A) hyperactive Parkin variants. These findings provide a framework to classify *Parkin* variants based on pathogenicity and suggest that several *pathogenic Parkin* variants represent promising targets for genotype-specific drug design.

Introduction

Parkinson's disease (PD) is the second most common neurodegenerative disease (1) and, although most PD cases are sporadic, a fraction are familial and caused by mutations in different genes (2). Mutations in the *Parkin* (*PARK2*) gene are the most common cause of autosomal recessive early-onset parkinsonism (EOPD) and are believed to result in a loss of Parkin protein function (3). *Parkin* variants include rearrangements and copy number variations, such as deletions and duplications of exons, as well as single nucleotide variants (SNVs) that cause missense, nonsense, or splice site mutations (4, 5). Of these, missense variants are the most frequently reported in PD patients (5) and, because they likely impede Parkin protein function rather than disrupting protein expression, may represent viable targets for therapies that enhance Parkin activity.

To envisage such genotype-specific therapies, the pathogenicity of the many *Parkin* variants in the population first needs to be determined. The American College of Medical Genetics and Genomics for Molecular Pathology (ACMG-AMP) has outlined five standard terminologies to describe variants identified in genes that cause Mendelian disorders (6). "*Pathogenic*" and "*likely pathogenic*" indicate a clear or very likely disease-causing effect of a variant, respectively. Conversely,"*likely benign*," and "*benign*" indicate variants that are not disease-causing. Variants that cannot be assigned to one of these four groups are designated as "*uncertain significance*". Over 200 *Parkin* missense variants have been deposited in public repositories (7-10). However, to date, only a minority have been clearly annotated based on formal criteria.

60 A clear assignment of a *Parkin* variant requires integrating different lines of evidence
61 that fall into two broad categories (6, 11). Clinical evidence consists of the association or
62 segregation of the variant with disease in human cohorts or within families with multiple
63 affected individuals. Functional evidence refers to the consequence(s) of the variant, using
64 experimental assays that measure biochemical and cellular properties as well as
65 computational algorithms that model the effect(s) of the variant based on protein structure
66 and function. Clinical evidence has a hierarchical relationship relative to functional
67 evidence and should prevail when a discrepancy or conflict arises between clinical and
68 functional observations (6, 11, 12).

69 Parkin is a basally autoinhibited E3 ubiquitin (Ub) ligase, which contains a N-terminal
70 Ubl domain, connected through a linker to four zinc-coordinating domains, RING0, RING1,
71 In-Between-RING (IBR), and RING2 (13), which form a core that we abbreviate as R0RBR.
72 Parkin is activated by PINK1, a mitochondrial kinase that is also implicated in EOPD (1).
73 PINK1 accumulates on damaged mitochondria upon depolarization, where it
74 phosphorylates nearby Ub(14-17). Parkin binds to phosphorylated Ub (pUb), which recruits
75 Parkin to mitochondria and facilitates PINK1 phosphorylation of the Parkin N-terminal
76 ubiquitin-like (Ubl) domain, which in turn fully activates Parkin (18-20). Parkin can then
77 ubiquitinate multiple outer mitochondrial membrane targets, triggering a feed-forward
78 amplification loop, that leads to the clearance of damaged mitochondria via autophagy
79 (mitophagy) (Reviewed in (21-23)). Some *Parkin* missense variants found in patients have
80 been shown to affect protein folding, Parkin autoubiquitination, protein-protein interactions
81 or recruitment to mitochondria (24-31). However, as the pathogenic nature of most of these

82 variants were not clear, the disease relevance of the functional alteration remained to be
83 determined.

84 Here, we characterized all *Parkin* missense variants found in public databases
85 according to ACMG-AMP criteria. We then used a cell-based assay to quantify Parkin-
86 mediated mitophagy and Parkin protein levels. We also applied structural simulation to
87 explore the mechanism underlying the observed functional alterations. Integrating these
88 data, we find that only a minority of *Parkin* variants can be considered *pathogenic*.
89 Interestingly, we identify several naturally-occurring *Parkin* variants in the population that
90 increase mitophagy in cells. Remarkably, such hyperactive *Parkin* variants were able to
91 rescue the impaired function of several common *pathogenic Parkin* variants. Our study
92 suggests that several *pathogenic* PD-linked *Parkin* mutations represent promising targets
93 amenable to genotype-specific drug design.

94 Results

95 Most *Parkin* missense variants lack sufficient clinical 96 evidence to determine pathogenicity

97 To classify *Parkin* variants, we utilized Sherloc (semiquantitative, hierarchical
98 evidence-based rules for locus interpretation), a classification framework that translated
99 the ACMG-AMP standards to a set of discrete but related rules with refined weights (11).
100 Clinical evidence was examined first, as it most directly describes disease (11). Briefly,
101 data from population databases, including minor allele frequency (MAF) and homozygote
102 counts, and clinical records in PD-specific databases that report PD patients or unaffected

103 family members carrying missense variants in *Parkin*, were examined to assign weighted
104 points as pathogenic or benign to each variant (Supplementary figure 1). The pathogenic
105 points and benign points were summed-up separately and compared to preset thresholds
106 to assign the variants with one of the five ACMG-AMP categories (Supplementary figure
107 2).

108 From the PD-specific databases, PDmutDB (5, 9) and MDSgene (4, 7), we identified
109 a total of 75 *Parkin* missense variants reported in PD patients (Figure 1). Most were absent
110 or very rare in the control cohorts from the original reports, possibly due to the small sizes
111 of the control cohorts. Therefore, we searched the 75 variants in public population
112 databases and found that 51 of them were reported in dbSNPs (10) and in the Exome
113 Aggregation Consortium (ExAC), including high-quality variant calls across 60,706 human
114 exomes (8) (Figure 1). From ExAC, we also found an additional 164 *Parkin* missense
115 variants (Figure 1). The classification of the missense variants using clinical evidence
116 allowed us to clearly designate thirteen variants with PD as *pathogenic* or *likely pathogenic*
117 and ten variants as *likely benign* or *benign* (Figure 1). In contrast, the large number of
118 remaining variants lacked sufficient data to be assigned to either the *benign* or *pathogenic*
119 categories and were therefore designated as of *uncertain significance* (Figure 1).

120 All ten *likely benign* or *benign* variants were reported in both PD patients as well as in
121 general population cohorts (Figure 1, 2A-B). Thus, we conclude that their presence in
122 patients was due to their high prevalence and not pathogenicity. Indeed, five of them had
123 high MAFs in ExAC, and one variant, p.M192L was absent from ExAC but common in
124 dbSNP. Their MAF or maximum MAF exceeded the cutoff considered as *high* in the Sherloc

125 classification system (Supplementary figure 1 and (11)). Four variants had MAFs in ExAC
126 that were considered *somewhat high*, which is inconsistent with MAF spectrum of over 95%
127 of previously well-characterized pathogenic variants from Sherloc (Supplementary figure 1
128 and (11)). All these variants were observed as homozygous in more than two individuals in
129 the ExAC database, which provided additional corroborating evidence that they were
130 *benign* or *likely benign*. Moreover, p.R334C was found as homozygous or compound
131 heterozygous in unaffected family members from two independent families (32) (33),
132 leading to assignment of four additional benign points (Figure 2B). Finally, none of the 10
133 variants showed segregation with PD in families, in further support of their lack of
134 pathogenicity. Thus, taken together, we suggest that these *likely benign* or *benign* variants
135 are not responsible for PD in the reported patients.

136 Thirteen variants were designated as *pathogenic* or *likely pathogenic* based on clinical
137 evidence (Figure 2A-B). Most were absent or very rare in the population databases. They
138 were reported as homozygous or compound heterozygous in several patients from multiple
139 families. These two lines of evidence largely accounted for their designations as
140 *pathogenic* or *likely pathogenic*. Of note, the MAFs of two variants, p.R275W and p.G430D
141 were somewhat high in ExAC. However, their strong segregation with PD in multiple
142 families supported their classification as *likely pathogenic* (11).

143 Although multiple missense variants were reported in PD patients, for the majority,
144 clinical evidence alone was not sufficient to support their pathogenicity (Figure 1). Most
145 were found only as heterozygous in PD patients, which did not contribute any points
146 towards pathogenicity (Figure 3A-B and data not shown when their functional analysis was

147 not performed). Thirteen were reported as homozygous or compound heterozygous in
148 patients (Figure 3A). Six of them were absent or rare in the population database (p.C289G,
149 p.K161N, p.C253F, p.C418R, p.W54R, p.E444Q). However, as only one case was found
150 per variant, the total points assigned did not exceed the threshold to designate them as
151 *likely pathogenic* (Figure 3A-B). Seven of them (p.T240M, p.P437L, p.R33Q, p.E310R,
152 p.P37L, p.R234Q and p.D280N) were reported in multiple cases but had *somewhat high*
153 MAF in ExAC (Figure 3A). From segregation analysis (Supplementary figure 1), p.T240M
154 showed strong segregation with PD in multiple families. It also was reported as compound
155 heterozygous in an unaffected family member (34). Thus, the benign and pathogenic points
156 for p.T240M exceeded the respective thresholds as *likely benign* or *likely pathogenic*
157 (Figure 3B). The contradictory criteria for benign and pathogenic assigned it as of *uncertain*
158 *significance*, suggesting a low-penetrance variant, a genetic modifier or that additional
159 corroborating evidence is require for more definitive assignment (Supplementary figure 2).
160 p.P437L and p.R33Q showed moderate and weak segregation with PD, respectively, and
161 the remaining four variants showed no clear segregation, leaving each below the *likely*
162 *pathogenic* threshold (Figure 3A-B).

163 Finally, none of the variants found only in the population databases were reported in
164 PD cases to support their pathogenicity (Figure 3A-B and data not shown when their
165 functional analysis was not performed). However, because their MAFs did not exceed the
166 cutoff for the high range, and none of the variants were found as homozygous in more than
167 two individuals from ExAC, they also lacked enough evidence to be designated as *likely*

168 *benign* or *benign* and were thus designated as variants of *uncertain significance* (Figure
169 1).

170 *Parkin* variants can be classified functionally in cells

171 Next, to determine the effects of the variants on Parkin function, we employed a cell-
172 based assay to monitor and quantify mitophagy dynamically using fluorescence-activated
173 cell sorting (FACS) in U2OS cells stably expressing inducible mt-Keima, a pH-sensitive
174 fluorescent protein that is targeted to mitochondria and exhibits a large shift in its emission
175 wavelength upon engulfment in the acidic compartment of lysosomes. The cells also
176 transiently expressed either wildtype (WT) Parkin or one of the Parkin variants fused to
177 GFP and the shift in mt-Keima emission was measured upon mitochondrial depolarization
178 with CCCP (Supplementary Figure 3A). The GFP intensity in untreated cells was also
179 quantified as a measure of steady-state Parkin protein stability (Supplementary Figure 3B).
180 The level of CCCP induced Parkin-mediated mitophagy and GFP intensity of the Parkin
181 variants were normalized to that of WT Parkin.

182 We analyzed all the variants that were designated clinically as *pathogenic* or *likely*
183 *pathogenic*, *benign* or *likely benign*, and an additional twenty-eight variants designated as
184 of *uncertain significance.* These variants represented the most common missense variants
185 reported in human population from public databases. Moreover, they were reported in 283
186 out of 309 families or unrelated patients in PD-specific databases. The thirteen *Parkin*
187 variants classified as *pathogenic* or *likely pathogenic* based on clinical evidence (Figure
188 2A and 2B) all showed significantly decreased mitophagy (Figure 2C). Seven variants

189 (p.C253Y, p.R42P, p.C441R, p.C212Y, p.C238W, p.V56E and p.R275W) also showed
190 decreased GFP intensity (Figure 2C), suggesting reduced protein stability. Of these, all the
191 variants in the R0RBR formed inclusions to different degrees, detected by fluorescence
192 microscopy (Supplementary figure 4). In contrast, the p.R42P and p.V56E variants in the
193 Ubl domain showed lower overall GFP intensity without visible inclusions. Thus, for a
194 subset of *pathogenic* and *likely pathogenic Parkin* variants, the observed defects in
195 mitophagy are likely to stem from abnormal protein folding and reduced protein stability. In
196 contrast, all ten *Parkin* variants classified as *benign* and *likely benign* based on clinical
197 evidence (Figure 2A and 2B), exhibited similar GFP intensity as WT and most, with three
198 exceptions, also exhibited WT levels of Parkin-mediated mitophagy (Figure 2C). p.Q34R
199 and p.A46T displayed decreased mitophagy, whereas p.R334C showed an almost three-
200 fold increase (Figure 2C). Of the twenty-eight variants classified as of *uncertain*
201 *significance* based on clinical evidence (Figure 3A and 3B), fourteen displayed similar GFP
202 intensity and mitophagy as WT Parkin (Figure 3C). Nine displayed impaired mitophagy,
203 three of which also showed decreased GFP intensity. Surprisingly, five variants showed
204 increased mitophagy.

205 The wide range of changes in Parkin levels and mitophagy prompted us to ask whether
206 we could classify the different variants into discrete groups. Variants that significantly
207 decreased Parkin protein levels and mitophagy were assigned to Group 1 (Figure 4A and
208 Supplementary table 1). Variants that severely (0-30% of WT) or moderately (30-60% of
209 WT) reduced Parkin-mediated mitophagy but that displayed normal protein levels were
210 assigned to Groups 2 and 3, respectively. Group 4 consisted of variants that were similar

211 to WT whereas Group 5 consisted of variants with increased (>140% of WT) Parkin-
212 mediated mitophagy. Interestingly, all the *pathogenic* or *likely pathogenic* variants,
213 classified based on clinical evidence, were assigned to group 1 or 2 whereas all the *benign*
214 or *likely benign* variants fell into group 3, 4, or 5 (Figure 4B). In all the PD case reports we
215 analyzed with *Parkin* variants, almost half displayed normal or hyperactive function, falling
216 into group 4 and 5 (Figure 4C). This suggests that caution must be exercised when
217 assigning causality to *Parkin* variants reported only in case reports as this may lead to an
218 overestimation of the prevalence of Parkin-related PD.

219 We next examined which lines of clinical evidence were most strongly correlated with
220 functional alterations. Among the variants that segregated with PD in families
221 (Supplementary figure 1C), all but one (p.R33Q) severely altered Parkin function and were
222 assigned to groups 1 or 2 (Figure 4D-E). However, it is important to note that segregation
223 analysis was only possible in ~30 families, as most reports only involved single cases or
224 case series (Figure 4F). Conversely, variants that were reported as homozygotes in ExAC
225 were frequent in Groups 3, 4 and 5 and were not assigned to Groups 1 or 2 (Figure 4G-I).
226 Finally, the observation of homozygous or compound heterozygous variants in isolated PD
227 patients (Supplementary figure 5A-C) and a low MAF of variants in population databases
228 (Supplementary figure 5D-F) would each be expected to suggest pathogenicity. However,
229 neither of these criteria correlated with the distribution of variants across our 5 functional
230 groups. Thus, taken together, our data show that variants that segregate with disease in
231 families impair Parkin function (Groups 1 and 2) whereas variants that occur as
232 homozygotes in ExAC do not severely reduce Parkin function (Groups 3, 4 and 5).

233 # Integration of clinical and functional evidence refines
234 # the classification of *Parkin* variants

235 Next, we devised a scoring scheme, based on Sherloc, to assign benign or pathogenic
236 points (Supplementary figure 6), according to the functional group to which the *Parkin*
237 variants were assigned in the cellular assays (Figure 4). The pathogenic points and benign
238 points were then added to the corresponding points from clinical evidence (Figure 2B, 3B,
239 and Supplementary figure 1) in order to obtain combined *pathogenic* and *benign* scores
240 from all evidence for each variant (Figure 5A and B).

241 Using these combined clinical and functional scores, all the *likely pathogenic* variants
242 from clinical evidence were reclassified as *pathogenic* (Figure 5A). Additionally, three *likely*
243 *benign* variants were reclassified as *benign* (Figure 5A). Most of the variants of *uncertain*
244 *significance* were reclassified as *likely benign*, while six (including p.T240M) were
245 reclassified as *pathogenic* and 9 remained of *uncertain significance* (Figure 5B). In
246 summary, all the variants that caused functional alterations assigned to groups 1 and 2, as
247 measured in our experimental assay, were reclassified as *pathogenic* whereas most
248 variants assigned to functional groups 3, 4 and 5 were reclassified as either *benign* or *likely*
249 *benign* (Figure 5C).

250 # Structural analysis of *Parkin* variants reveals
251 # pathogenic mechanisms

252 As the structure of Parkin is known, we simulated the effects of variants on the
253 reported crystal structures of Parkin to understand the mechanism underlying the

254 functional change. The autoinhibited Parkin, pUb-bound Parkin, p-Ub-bound phospho-
255 Parkin, pUb -E2 enzyme-bound phospho-Parkin structures were used as they represented
256 Parkin in different states of activation (19, 20, 35, 36).

257 Most variants in functional groups 1, 2 and 3 introduced clashes or altered interactions
258 with nearby residues in at least one of the Parkin structures. In contrast, most variants in
259 Group 4, which displayed similar function as WT Parkin, introduced no major clashes and
260 did not affect interactions (Figure 6A-B). However, mild clashes were observed in a few
261 cases, suggesting that some degree of clashing could be tolerated and possibly
262 compensated by local conformation changes to maintain overall protein function. For
263 example, three variants at Arg42 were analyzed. Mutation of Arg42 to proline introduced
264 massive clashes, whereas substitution to histidine introduced mild clashes and there was
265 no clash introduced by substitution to cysteine (Supplementary figure 7). Congruently, only
266 p.R42P was classified as *pathogenic* based on clinical criteria (Figure 2B and 3B) and
267 impaired functionally in cell-based assays (Figure 2C and 3C), consistent with this mutation
268 actually unfolding the domain (25, 37).

269 The steric consequences of variants in Groups 1 and 2 are likely to disrupt several
270 different aspects of Parkin function (Figure 6C). Seven variants involve cysteines that
271 coordinate zinc, and their mutations would result in the overall misfolding of the Parkin
272 protein (35). Five variants impaired key motifs mediating ubiquitination of substrates,
273 including steric clashes with the E2 binding site on RING1 (p.T240R and p.T240M), and
274 residues implicated in thioester transfer of Ub in the catalytic RING2 domain (p.T415N,
275 p.G430D, p.C431F) (38). These types of alterations are likely to cause a complete loss of

276 Parkin function in either PINK1-Parkin mediated mitophagy or other potential Parkin
277 pathways. Four variants specifically disrupted the conformational change that occurs
278 during activation by PINK1. p.K161N and p.K211N introduced no or mild steric clashes,
279 but mutation of the basic lysine to neutral asparagine eliminate the interaction with the
280 acidic phosphate in pUbl (Supplementary figure 8A and (19, 20)). p.G284R introduces
281 major clashes with pUb, thus impairing binding and recruitment to mitochondria
282 (Supplementary figure 8B). p.R275W disrupts interaction with the helix that mediates pUb
283 binding (Supplementary figure 8C). This would destabilize the protein, and indeed the
284 protein levels of R275W are lower than WT (Figure 2C). This helix becomes more exposed
285 following pUb binding and may be involved in the allosteric release of the Ubl (19, 20), and
286 Arg275 was also suggested to bind ubiquitin charged on an E2 enzyme (36), suggesting a
287 combined effect of impaired activation and protein destabilization. The clashes caused by
288 p.R42P and p.V56E are predicted to misfold the Ubl domain and thus destabilize the
289 protein, as demonstrated earlier for p.R42P which was found to be insoluble (25).
290 Meanwhile they may also hinder conformational change during activation by preventing
291 Ubl phosphorylation and the binding of pUbl on RING0. One variant, p.P437L, introduced
292 very mild clashes in RING2 in the structure, and the exact molecular mechanism of
293 p.P437L in causing decreased mitophagy was unclear.

294 Several variants in functional Group 3 that moderately decreased Parkin-mediated
295 mitophagy might also act by hindering Parkin activation by PINK1. p.A46T could disrupt
296 the interaction of pUbl with RING0 (Supplementary figure 8D). Arg104 is located in the
297 newly identified activation element (ACT) in the linker (20), which binds RING0 and helps

298 stabilize the interaction with pUbl. p.R104W disrupted a short helix in the ACT and induced
299 clashes with the pUbl (Supplementary figure 8E and(20)). p.G359D disrupted the glycine-
300 rich loop in the IBR domain that interacts with pUb (Supplementary figure 8F). These
301 clashes may be compensated by minor local conformation changes, and thus lead to
302 milder disruptions in mitophagy and protein stability.

303 Structure-guided *designer* hyperactive Parkin mutants 304 can rescue mitophagy in pathogenic variants

305 We next hypothesized that some of the *pathogenic* variants may represent targets for
306 genotype-specific therapy. As a proof of concept, we introduced two artificially designed
307 mutations, W403A and F146A, which destabilized the REP (repressor element of
308 Parkin):RING1 and the RING0:RING2 interfaces, respectively. Both of these mutations
309 have been shown to accelerate mitophagy by promoting the conformational changes that
310 occur at these interfaces during Parkin activation by PINK1 (35, 39). We tested whether
311 these *hyperactive* mutations could rescue the mitophagy defects seen in the *pathogenic*
312 Parkin variants. As reported previously, mutating F146A or W403A alone enhanced
313 mitophagy compared to WT Parkin (Figure 7A) (14, 35, 39). Remarkably, introducing
314 F146A or W403A *in cis* with p.R42P, p.V56E, p.K161N, p.K211N, p.R275W p.P437L or
315 p.T240M rescued mitophagy (Figure 7A). Variants p.R42P, p.V56E and p.R275W each
316 lower Parkin levels, likely by disrupting protein stability (Figure 2C). However, introduction
317 of F146A or W403A did not restore Parkin levels to WT (Supplementary figure 9),
318 suggesting the rescue of mitophagy was mediated by Parkin activation *per se* rather than

319 by enhancing Parkin protein stability. The *pathogenic* variants p.K161N and p.K211N are
320 involved in binding the pUbl during activation (19, 20). The fact that both these variants
321 can be rescued by F146A or W403A suggests that destabilization of the REP:RING1 or
322 the RING0:RING2 interface can bypass the tethering of the Ubl to RING0, which occurs
323 during Parkin activation.

324 In contrast, neither F146A nor W403A could rescue any of the 7 *pathogenic* cysteines
325 variants involved in zinc coordination (Figure 6C). This is not surprising as mutating these
326 cysteines are predicted to severely disrupt overall Parkin folding and stability (Figure 2C
327 and3C). Similarly, variants that disrupted key catalytic or activation sites could not be
328 rescued. For instance, neither F146A nor W403A could rescue p.T415N, p.G430D or
329 p.C431F, which are involved in thioester transfer of Ub onto the catalytic RING2 domain
330 (Figure 6C). Not surprisingly, p.G284R also could not be rescued as it disrupts binding to
331 pUb, which is an essential receptor for recruiting Parkin to damaged mitochondria (40).
332 Interestingly, whereas both p.T240M and p.T240R are predicted to interfere with E2 Ub-
333 conjugating enzyme binding to RING1 (Figure 6C) and showed similar severe defects in
334 mitophagy (Figure 2C and 3C), only the former could be rescued by F146A or W403A
335 (Figure 7A). Both variants created clashes in the E2 binding site (Supplementary figure 10).
336 However, arginine created a positive charge at the interface, increasing the electrostatic
337 repulsion of E2. Methionine is less bulky and neutral, and its flexibility could allow some
338 weak interactions with E2 to remain, perhaps explaining its rescue by F146A or W403A.

339 Overall, the defects in mitophagy of seven of the 19 *pathogenic* variants could be
340 rescued by the designed activating mutations. These seven variants are responsible for

341 over 75% of reported PD patients carrying *pathogenic* missense variants (Figure 7B) and
342 were the most frequent *pathogenic* missense variants in the general population (Figure
343 7C). Mimicking the effects of F146A or W403A could therefore be useful for starting point
344 for designing a treatment for patients with PD caused by these *Parkin* variants.

345 Characterization of naturally-occurring hyperactive 346 Parkin variants

347 We identified 6 naturally-occurring variants that, considering all the evidence, were
348 classified as *likely benign* or *benign* and showed enhanced Parkin-mediated mitophagy.
349 The Parkin structure shows that Arg234 and Arg256 are located at the interface between
350 the REP and RING0. The p.R234Q and p.R256C variants are predicted to destabilize the
351 interface, thus mimicking the W403A *designer* mutant used above (Supplementary Figure
352 11A). Additionally, p.M458L may destabilize the RING0:RING2 interface, mimicking the
353 effects of our other *designer* mutation, F146A (Supplementary Figure 11B). Thus, 3 of the
354 6 naturally-occurring variants are likely to activate Parkin via mechanisms akin to those
355 involved in the hyperactive mutants designed previously, based on structural predictions
356 (39). Because these variants occur naturally in the population, our findings demonstrating
357 rescue of mitophagy suggest that targeting these sites and mechanisms are likely to be
358 tolerated and potentially therapeutic in PD. p.P37L also moderately increased Parkin-
359 mediated mitophagy, but the structural basis of the increased activity was unclear, as this
360 variant does not create any steric clash and thus should not affect interactions of the Ubl
361 with RING1 or interactions of the pUbl with RING0 (Supplementary Figure 11C and 11D).

362 Mutation of R334 to a cysteine could affect the coordination of a nearby zinc in the IBR,
363 which may stabilize the interaction with phospho-ubiquitin and thereby enhance Parkin
364 activity (Supplementary Figure 11E).

365 Finally, unlike the 5 other naturally-occurring hyperactive variants, p.V224A has not
366 been reported in PD patient databases and showed the highest (almost 3-fold above WT)
367 Parkin-mediated mitophagy activity (Figure 3C). The Val224 residue is localized in the pUb
368 binding pocket, with its side-chain facing towards the phosphorylated Ser65 residue of pUb
369 and the mutation to alanine could modulate the affinity of Parkin for phospho-ubiquitin
370 (Supplementary Figure 11F). We therefore examined the ability of hyperactive p.V224A to
371 rescue the defects in mitophagy of the *pathogenic* variants. Introducing the p.V224A
372 variant *in cis* did not affect the protein level of most *pathogenic* variants, except for
373 p.G284R (Figure 8A). This may stem from an additive destabilizing effect of the double
374 mutant on Parkin folding as both p.V224A and p.G284R are located within the same pUb
375 binding motif. Introducing the p.V224A variant partially rescued the mitophagy defects of
376 p.R42P, p.V56E and p.K161N (Figure 8B). How the predicted effects of V224A on pUb-
377 binding could partially compensate for defects in Ubl- and pUbl-mediated activation by
378 p.R42P, p.V56E and p.K161N remains to be elucidated. Moreover, the rescue of p.K161N
379 but not p.K211N cannot be easily explained since both are predicted to interfere with pUbl
380 binding (Supplementary figure 7A) and tethering of the Ubl to RING0 during activation (19,
381 20). Similarly, p.V224A could not rescue the mitophagy deficit in p.R275W and p.G284R
382 variants, predicted to disrupt pUb binding, nor could it rescue any of the remaining
383 *pathogenic* variants (Figure 8B). Thus, compared with F146A or W403A, p.V224A was less

384 effective at rescuing the *pathogenic* variants, suggesting that the pUb-binding site may be
385 a less promising target than releasing the autoinhibited conformation of Parkin for
386 activating mitophagy.

387 Discussion

388 *Parkin* mutations are the most common cause of recessive early-onset PD (EOPD)
389 (3). Although *Parkin* loss-of-function is well established in EOPD (4, 41), causality for any
390 given missense variant has been more difficult to ascertain. In this study, we have
391 integrated clinical, experimental and structural modeling approaches to map out the
392 landscape of *Parkin* variants in the general population and in PD patients. Our hope is that
393 this work will help provide a more cohesive framework to guide basic science studies
394 exploring the molecular and cellular functions of the *PINK1/Parkin* pathway and to guide
395 clinicians caring for patients carrying specific *Parkin* variants. We also hope that the work
396 will inform structure-based drug design to develop Parkin activators and help guide Parkin
397 allele- and genotype-specific clinical studies.

398 For the over 200 *Parkin* variants reported in public databases (4, 5, 8), we found that
399 only a minority of variants could be clearly designated as *likely pathogenic*, *pathogenic*,
400 *likely benign* or *benign* based on clinical evidence alone. While this may not seem
401 surprising for variants found only in population databases such as ExAC, where
402 accompanying clinical information is scant, we found a similar situation for variants
403 reported in patients. Indeed, 52 out 75 variants reported in PDmutDB and MDSgene
404 remained of *uncertain significance* after having been subjected to the Sherloc algorithm,

405 the variant classification framework derived from ACMG standards that we used in this
406 study. The overarching message from these observations is that the mere presence of
407 *Parkin* variants in PD patients, PD kindreds or PD-specific databases should be interpreted
408 with caution and not automatically taken to imply pathogenicity. Rather, we propose that
409 clinical evidence available for new variants should be subjected to the same rigorous
410 classification scheme presented here to determine pathogenicity.

411 In addition to analyzing clinical evidence, we extensively characterized the cellular
412 effects of the 51 *Parkin* variants most commonly found in patient and population
413 sequencing databases (Over 90% of all PD patients carrying Parkin missense variants in
414 disease databases; Sum of MAF as 28.177% out 28.533% in ExAC). Using mitophagy and
415 steady-state Parkin protein levels as readouts in a flow cytometry-based assay, we were
416 able to classify the variants into 5 functional groups. To our knowledge, a systematic
417 analysis integrating clinical evidence with cellular function, on this scale, has not been
418 reported previously for *Parkin* (24-31). Notably, all the variants designated as *pathogenic*
419 or *likely pathogenic* based on clinical evidence also displayed severe mitophagy defects in
420 cells (functional groups 1 and 2). Conversely, all variants designated clinically as *benign* or
421 *likely benign* displayed mitophagy function in the WT range or showed only a slight
422 reduction (functional groups 3, 4 and 5). While this may seem *a priori* as self-evident,
423 several alternative functions of Parkin in cells have been proposed and the role of
424 mitophagy in PD has yet to be definitively established (21, 22, 42, 43). Thus, while this
425 work does not refute the biological importance of such alternative functions, the tight
426 correlation between the clinical impact of the variants and their effects on mitophagy

427 provides further evidence that mitophagy can be used as a robust and disease-relevant
428 readout of Parkin function that likely reflects a key pathogenic process in PD.

429 Assignment of the *Parkin* variants to functional groups in cells allowed us to determine
430 which clinical features best correlate with and could be used to predict pathogenicity.
431 Segregation of variants with PD in families turned out to be very strongly associated with
432 defects in mitophagy, whereas variants that occurred as homozygotes in ExAC never
433 displayed defects in mitophagy in cells. Therefore, we propose that these two clinical
434 criteria be used as strong predictors of pathogenicity of *Parkin* variants. In contrast, neither
435 the number of variants in PD patients nor the MAF in population databases correlated with
436 cellular function, suggesting that these clinical criteria would not be useful predictors of
437 pathogenicity. Perhaps more importantly, integrating clinical with functional evidence from
438 cells allowed us to re-assign 19 of the 28 variants, designated as of *uncertain significance*
439 based on clinical evidence alone, to one of the benign and pathogenic categories. It also
440 allowed us to reclassify 6 of the "*likely*" variants to their respective more definitive *benign*
441 and *pathogenic* categories. Together, these findings attest to the power of using this sort
442 of iterative combined clinical and experimental approach to stratify variants.

443 Beyond stratification, given what is already known about the structure and function of
444 the Parkin protein, the work enables in-depth mechanistic exploration of how *pathogenic*
445 variants can lead to dysfunction. This is something that has been sorely lacking and may
446 have important implication for how best to target Parkin and design activator for future
447 therapy. As one might expect, most missense variants that led to severe defects in
448 mitophagy (Functional groups 1 and 2) introduced clashes with nearby residues. Almost

449 all the variants that also led to reduced steady-state Parkin levels (Functional group 1)
450 introduced major clashes, likely leading to protein destabilization and, for several, the
451 formation of inclusions in cells. These inclusions-forming variants occurred in zinc-
452 coordinating cysteine residues within RING domains, which are required for proper protein
453 folding. Additional variants are predicted to impede pUb-binding, E2-binding, Ubl folding,
454 the RING0-pUbl interface or Parkin catalytic activity centered around residue C431. In
455 contrast, variants that led to only minor or no changes in Parkin function in cells (Functional
456 groups 3 and 4), for the most part did not introduce clashes or only minor clashes that likely
457 could be tolerated or compensated by local rearrangements in nearby residues. Taken
458 together, the important point is that, for most of the *pathogenic* variants, the mechanisms
459 by which they interfere with function can be rationalized based on the Parkin structure.

460 As an important proof of concept, we showed that the function of several pathogenic
461 *Parkin* variants, defective in mitophagy in cells, could be rescued when expressed *in cis*
462 with mutations that we had previously designed to enhance Parkin activity, based on its
463 structure(35, 39). Notably, many of the most commonly occurring variants were the ones
464 that could be rescued, something that bodes well for patients carrying these variants,
465 should a therapeutic mimicking W403A or F146A become available. The variants that could
466 be rescued could be stratified according to structure and mechanism. For instance,
467 alterations in residues involved in zinc coordination, in catalytic activation or in pUb-binding
468 could not be rescued. In contrasts, alterations in residues involved in Ubl folding or in the
469 pUbl-RING0 interface in the active Parkin structure could be fully rescued. Similarly,
470 p.R104W in the ACT motif, which is predicted to destabilize the pUbl-RING0 interface led

471 to only a minor defect in mitophagy. Together, these data suggest that binding of the pUbl
472 to RING0, as seen in the recent crystal structures of the active configuration of Parkin(19,
473 20), may not be absolutely required for activation and could potentially be bypassed by a
474 therapeutic that disrupted the REP-RING1 or the RING0-RING2 interfaces. Interestingly,
475 both p.T240R and p.T240M variants in the E2-binding site of RING1, abolish mitophagy in
476 cells. However, while p.T240R could be rescued, p.T240M could not. This likely stems from
477 the additional electrostatic effects of the arginine compared to the methionine substitution
478 in repulsing the E2 enzyme. Congruently with these structural and functional findings
479 suggesting that p.T240R is more severe, clinical evidence led to the assignment of
480 p.T240R as *likely pathogenic* whereas p.T240M was classified as *of uncertain significance*.
481 This highlights the importance of carefully considering clinical, functional and structural
482 data for each variant as they may have profound implications, not only for prognosis but
483 also for patient stratification for therapy.

484 One of the most surprising findings of our study was that several naturally-occurring
485 variants exhibited a 1.5- to almost 3-fold enhancement Parkin-mediated mitophagy in our
486 assay. This could not simply be explained by increased Parkin protein levels or by the fact
487 that our assay involved overexpression. Indeed, except for certain pathogenic variants that
488 destabilized Parkin, most variants, including these hyperactive one, displayed steady-state
489 levels that were within a narrow window around WT. These hyperactive variants provide
490 an important proof of principle that there are, presumably healthy, people out there in the
491 population living with enhanced Parkin activity. While all of these variants were classified
492 clinically as either *benign* or *of uncertain significance*, because they are so rare, it is unlikely

493 that it will be possible to test at a population level whether they are in fact protective against
494 PD. On a mechanistic level, 3 of the 6 naturally-occurring hyperactive variants likely act by
495 disrupting the REP-RING1 or RING0-RING2 interfaces, similarly to and to the same extent
496 (roughly 1.5-fold) as p.W403A and p.F146A, respectively. These findings add further
497 support to the idea that targeting these sites may be viable strategies for Parkin
498 enhancement. The most strongly activating variant was V224A, which increases mitophagy
499 by nearly 3-fold and occurs very near the site for pUb-binding. This was surprising as pUb-
500 binding serves as a critical receptor needed to recruit Parkin to mitochondria and, to date,
501 every reported mutation in this motif, abolished or dramatically reduced mitophagy.
502 Moreover, when expressed *in cis*, V224A partially rescued certain but not all the mutants
503 that were rescued by W403A and F146A. The mechanism by which V224A enhances
504 Parkin function and rescues defects elsewhere in the protein remain unknown. In the future,
505 it will be important to test whether this involves an enhancement in pUb-binding or some
506 other downstream allosteric effect. Similarly, it will be important to determine the
507 mechanisms by which the two remaining hyperactive variants, P37L and R334C, enhance
508 Parkin function. Moreover, as we only sampled 51 of the over 200 *Parkin* variants in the
509 population in this study, it is conceivable that other yet-to-be-discovered hyperactive
510 variants will provide further mechanistic insight into Parkin activation and help identify
511 additional therapeutic sites within the protein to target.
512
513

514 # Materials and methods

515 ## Classification of *Parkin* missense variants

516 We utilized Sherloc (semiquantitative, hierarchical evidence-based rules for locus
517 interpretation), a variant classification framework derived from ACMG standards (6) to
518 assign *Parkin* missense variants into five categories: *pathogenic*, *likely pathogenic*, *benign*,
519 *likely benign* and of *uncertain significance* (11). We considered two broad categories of
520 evidence for the classification, clinical and functional. The procedures for evaluating and
521 scoring these lines of evidence are summarized as root-decision trees in Supplementary
522 figures 1,2,6

523 For clinical evidence, information regarding missense variants in *Parkin* reported in
524 the population database ExAC (http://exac.broadinstitute.org/gene/ENSG00000185345)
525 and the disease-specific databases, PDmutDB (http://www.molgen.vib-ua.be/PDmutDB)
526 (5, 9), and MDSgene (http://www.mdsgene.org/) (7) were searched. We also searched
527 dbSNP (http://www.ncbi.nlm.nih.gov/snp) and the Exon variant server (EVS,
528 http://evs.gs.washington.edu/EVS/) for missense variants that were found in the disease
529 databases but not in ExAC. The homozygote count, MAF in ExAC and maximal MAF in
530 dbSNP, EVS and subpopulations in ExAC were calculated and used to assign points to the
531 variants according to the decision tree in Supplementary figure 1A. The clinical cases
532 reported in PDmutDB and MDSmutDB were evaluated according to the decision tree in
533 Supplementary figure 1B-C. The original references were traced back for the indexed
534 families or individuals reported in these databases. Indexed cases reported in both

535 databases cited from the same reference were only evaluated once. Indexed cases
536 reported in a more recent paper showing the same information (same number of family
537 members with same genotype and phenotype) as a case in an older reference were
538 considered as the same family and the older report was used.

539 For functional evidence, the effects of the variants in the cellular assay were assigned
540 points according to the decision tree in Supplementary figure 6. We imposed a 2.5-point
541 cap on functional evidence to ensure that functional data which lacked supporting clinical
542 evidence would not be sufficient on its own to reach the threshold required (3 benign points
543 or 4 pathogenic points; supplementary figure 2) to assign a variant into the *pathogenic* or
544 *benign* categories (11).

545 Cell culture, cloning and mutagenesis

546 Human osteosarcoma U2OS cells stably expressing GFP-Parkin were a gift from Dr.
547 Robert Screaton (Sunnybrook Research Institute). U2OS cells stably expressing mtKeima
548 were created by transfecting plasmid DNA using jetPRIME (Polyplus), followed by selection
549 with G418 for 2 weeks and sorting using flow cytometry (39). Cells were maintained in
550 DMEM supplemented with 10% fetal bovine serum (FBS), 4mM L-glutamine and 0.1%
551 Penicillin/Streptomycin, in a 37℃ incubator with 5% CO_2. All GFP-Parkin variants were
552 generated using PCR mutagenesis according to the manufacturer's protocol (Agilent
553 Technologies). Constructs were verified by sanger sequencing.

554 Mitophagy assay

555 Mitophagy was examined using FACS-based analysis of mitochondrially targeted mtKeima

556 (a gift from A. Miyawaki, Laboratory for Cell Function and Dynamics, Brain Science Institute,
557 RIKEN, Japan) as previously reported (39). Briefly, U2OS cells stably expressing
558 ecdysone-inducible mt-Keima were induced with 10 mM ponasterone A, transfected with
559 WT or variant GFP-Parkin for 24 h and treated with DMSO or 20 μM CCCP for 4 h. For
560 flow cytometry, cells were trypsin digested, washed and resuspended in PBS prior to their
561 analysis on an LSR Fortessa (BD Bioscience) equipped with 405 and 561 nm lasers and
562 610/20 filters (Department of Microbiology and Immunology Flow Cytometry Facility, McGill
563 University). Measurement of mtKeima was made using a dual-excitation ratiometric pH
564 calculation where pH 7 was detected through the excitation at 405nm and pH 4 at 561 nm.
565 For each untreated sample, 75,000 events were collected and single GFP-Parkin-positive
566 cells were subsequently gated for quantification of the geometric mean of the GFP signal
567 as a measure of steady-state Parkin protein levels. The value for each Parkin missense
568 variant was normalized to that for WT in each repeat. For each untreated and treated
569 sample, single GFP-Parkin-positive, mtKeima-405nm-positive cells were subsequently
570 gated. The percentage of cells with an increase in the 405nm:561nm ratio in mtKeima was
571 quantified. The percentage in treated cells minus the percentage in untreated cells was
572 calculated as the induced Parkin-mediated mitophagy. The induced mitophagy for each
573 Parkin missense variant was normalized to that for WT in each repeat. Data was analyzed
574 using FlowJo v10.1 (Tree Star).

575 # Modeling of Parkin Structures, Modifications and
576 Variants

577 The structures of human Parkin bound to phospho-ubiquitin (PDB 5N2W), rat parkin (PDB
578 4ZYN), human phospho-parkin bound to phospho-Ub (PDB 6GLC) and fly pParkin-pUb-
579 UbcH7 complex (PDB 6DJX) were analyzed using PyMOL version 1.5 (Schrödinger, New
580 York). Mutations and clashes were simulated using the mutagenesis wizard toolbox. The
581 presence of more than three simulated significant clashes (red disks) was taken to indicate
582 major clashes. One to three significant clashes (red disks) together with other slight
583 clashes (brown and green disks) were considered as minor clashes. Polar contacts within
584 4 Å distance of the residue were explored for characterizing interactions.

585 # Statistical analysis

586 For statistical analysis of mitophagy and protein levels, one-way analysis of variance
587 (ANOVA) with Bonferroni post-hoc tests were performed. To determine the ability of
588 hyperactive mutants to rescue *Parkin* variants, two-way analysis of variance (ANOVA) and
589 Bonferroni post-hoc test comparing row factors among the single or double mutations were
590 performed. *P<0.05; **P<0.01; ***P<0.001.

591 # Author contributions

592 W.Y. performed cloning, genetic analysis, and experiments in cells. E.J.M., M.Y.T. and A.I.K.
593 assisted with cloning and experiments in cells. Z.G-O. assisted with genetic analysis. J.-
594 F.T. assisted with all the structural simulations. W.Y., E.J.M., M.Y.T., Z.G-O, J.F.T. and E.A.F.
595 participated in the design of experiments, data analysis and preparation of the manuscript.

596 # Acknowledgements

597 We thank members from the Trempe and Fon labs, as well as Kalle Gehring for useful
598 discussion and comments. The flow cytometry work/ cell sorting was performed in the Flow
599 Cytometry Core Facility for flow cytometry and single cell analysis of the Life Science
600 Complex and supported by funding from the Canadian Foundation for Innovation. We
601 acknowledge support from Parkinson Society Canada (Basic Science Postdoctoral
602 Fellowship to W.Y.), and the Canadian Institutes of Health Research grant (FDN – 154301
603 (E.A.F.).

604

605 # References

606 1. Poewe W, Seppi K, Tanner CM, Halliday GM, Brundin P, Volkmann J, et al. Parkinson disease.
607 *Nature Reviews Disease Primers.* 2017;3:17013.
608 2. Klein C, and Westenberger A. Genetics of Parkinson's Disease. *Cold Spring Harbor perspectives*
609 *in medicine.* 2012;2(1):a008888.
610 3. Koros C, Simitsi A, and Stefanis L. Genetics of Parkinson's Disease: Genotype-Phenotype
611 Correlations. *International review of neurobiology.* 2017;132:197-231.
612 4. Kasten M, Hartmann C, Hampf J, Schaake S, Westenberger A, Vollstedt EJ, et al. Genotype-
613 phenotype relations for the Parkinson's Disease genes Parkin, PINK1, DJ1: MDSGene
614 Systematic Review. *Movement disorders : official journal of the Movement Disorder Society.*
615 2018.
616 5. Nuytemans K, Theuns J, Cruts M, and Van Broeckhoven C. Genetic etiology of Parkinson disease
617 associated with mutations in the SNCA, PARK2, PINK1, PARK7, and LRRK2 genes: a mutation
618 update. *Human mutation.* 2010;31(7):763-80.
619 6. Richards S, Aziz N, Bale S, Bick D, Das S, Gastier-Foster J, et al. Standards and guidelines for the
620 interpretation of sequence variants: a joint consensus recommendation of the American
621 College of Medical Genetics and Genomics and the Association for Molecular Pathology. *Genet*
622 *Med.* 2015;17(5):405-24.
623 7. Lill CM, Mashychev A, Hartmann C, Lohmann K, Marras C, Lang AE, et al. Launching the
624 movement disorders society genetic mutation database (MDSGene). *Movement disorders :*
625 *official journal of the Movement Disorder Society.* 2016;31(5):607-9.
626 8. Lek M, Karczewski KJ, Minikel EV, Samocha KE, Banks E, Fennell T, et al. Analysis of protein-
627 coding genetic variation in 60,706 humans. *Nature.* 2016;536:285.
628 9. Cruts M, Theuns J, and Van Broeckhoven C. Locus-specific mutation databases for
629 neurodegenerative brain diseases. *Human mutation.* 2012;33(9):1340-4.
630 10. Sherry ST, Ward MH, Kholodov M, Baker J, Phan L, Smigielski EM, et al. dbSNP: the NCBI
631 database of genetic variation. *Nucleic acids research.* 2001;29(1):308-11.
632 11. Nykamp K, Anderson M, Powers M, Garcia J, Herrera B, Ho Y-Y, et al. Sherloc: a comprehensive
633 refinement of the ACMG–AMP variant classification criteria. *Genetics In Medicine.*
634 2017;19:1105.
635 12. MacArthur DG, Manolio TA, Dimmock DP, Rehm HL, Shendure J, Abecasis GR, et al. Guidelines
636 for investigating causality of sequence variants in human disease. *Nature.* 2014;508(7497):469-
637 76.
638 13. Wenzel DM, Lissounov A, Brzovic PS, and Klevit RE. UBCH7 reactivity profile reveals parkin and
639 HHARI to be RING/HECT hybrids. *Nature.* 2011;474(7349):105-8.
640 14. Ordureau A, Sarraf Shireen A, Duda David M, Heo J-M, Jedrykowski Mark P, Sviderskiy
641 Vladislav O, et al. Quantitative Proteomics Reveal a Feedforward Mechanism for Mitochondrial
642 PARKIN Translocation and Ubiquitin Chain Synthesis. *Molecular Cell.* 2014.
643 15. Koyano F, Okatsu K, Kosako H, Tamura Y, Go E, Kimura M, et al. Ubiquitin is phosphorylated by
644 PINK1 to activate parkin. *Nature.* 2014.
645 16. Kazlauskaite A, Kondapalli C, Gourlay R, Campbell DG, Ritorto MS, Hofmann K, et al. Parkin is
646 activated by PINK1-dependent phosphorylation of ubiquitin at Serine65. *The Biochemical*
647 *journal.* 2014.

648 17. Kane LA, Lazarou M, Fogel AI, Li Y, Yamano K, Sarraf SA, et al. PINK1 phosphorylates ubiquitin
649 to activate Parkin E3 ubiquitin ligase activity. *The Journal of cell biology.* 2014;205(2):143-53.
650 18. Sauve V, Lilov A, Seirafi M, Vranas M, Rasool S, Kozlov G, et al. A Ubl/ubiquitin switch in the
651 activation of Parkin. *Embo j.* 2015;34(20):2492-505.
652 19. Sauvé V, Sung G, Soya N, Kozlov G, Blaimschein N, Miotto LS, et al. Mechanism of parkin
653 activation by phosphorylation. *Nature structural & molecular biology.* 2018;25(7):623-30.
654 20. Gladkova C, Maslen SL, Skehel JM, and Komander D. Mechanism of parkin activation by PINK1.
655 *Nature.* 2018;559(7714):410-4.
656 21. Pickrell AM, and Youle RJ. The Roles of PINK1, Parkin, and Mitochondrial Fidelity in Parkinson's
657 Disease. *Neuron.* 2015;85(2):257-73.
658 22. Panicker N, Dawson VL, and Dawson TM. Activation mechanisms of the E3 ubiquitin ligase
659 parkin. *The Biochemical journal.* 2017;474(18):3075-86.
660 23. Pickles S, Vigié P, and Youle RJ. Mitophagy and Quality Control Mechanisms in Mitochondrial
661 Maintenance. *Current Biology.* 2018;28(4):R170-R85.
662 24. Sriram SR, Li X, Ko HS, Chung KKK, Wong E, Lim KL, et al. Familial-associated mutations
663 differentially disrupt the solubility, localization, binding and ubiquitination properties of parkin.
664 *Human molecular genetics.* 2005;14(17):2571-86.
665 25. Hampe C, Ardila-Osorio H, Fournier M, Brice A, and Corti O. Biochemical analysis of Parkinson's
666 disease-causing variants of Parkin, an E3 ubiquitin-protein ligase with monoubiquitylation
667 capacity. *Human molecular genetics.* 2006;15(13):2059-75.
668 26. Matsuda N, Kitami T, Suzuki T, Mizuno Y, Hattori N, and Tanaka K. Diverse Effects of Pathogenic
669 Mutations of Parkin That Catalyze Multiple Monoubiquitylation in Vitro. *Journal of Biological*
670 *Chemistry.* 2006;281(6):3204-9.
671 27. Fiesel FC, Caulfield TR, Moussaud-Lamodiere EL, Ogaki K, Dourado DF, Flores SC, et al.
672 Structural and Functional Impact of Parkinson Disease-Associated Mutations in the E3
673 Ubiquitin Ligase Parkin. *Human mutation.* 2015;36(8):774-86.
674 28. Safadi SS, Barber KR, and Shaw GS. Impact of Autosomal Recessive Juvenile Parkinson's Disease
675 Mutations on the Structure and Interactions of the Parkin Ubiquitin-like Domain. *Biochemistry.*
676 2011;50(13):2603-10.
677 29. Wang C, Tan JM, Ho MW, Zaiden N, Wong SH, Chew CL, et al. Alterations in the solubility and
678 intracellular localization of parkin by several familial Parkinson's disease-linked point mutations.
679 *Journal of neurochemistry.* 2005;93(2):422-31.
680 30. Narendra DP, Jin SM, Tanaka A, Suen D-F, Gautier CA, Shen J, et al. PINK1 Is Selectively Stabilized
681 on Impaired Mitochondria to Activate Parkin. *PLoS Biol.* 2010;8(1):e1000298.
682 31. Geisler S, Holmstrom KM, Skujat D, Fiesel FC, Rothfuss OC, Kahle PJ, et al. PINK1/Parkin-
683 mediated mitophagy is dependent on VDAC1 and p62/SQSTM1. *Nature cell biology.*
684 2010;12(2):119-31.
685 32. Chaudhary S, Behari M, Dihana M, Swaminath PV, Govindappa ST, Jayaram S, et al. Parkin
686 mutations in familial and sporadic Parkinson's disease among Indians. *Parkinsonism & related*
687 *disorders.* 2006;12(4):239-45.
688 33. Biswas A, Gupta A, Naiya T, Das G, Neogi R, Datta S, et al. Molecular pathogenesis of Parkinson's
689 disease: Identification of mutations in the Parkin gene in Indian patients. *Parkinsonism &*
690 *related disorders.* 2006;12(7):420-6.
691 34. Deng H, Le WD, Hunter CB, Ondo WG, Guo Y, Xie WJ, et al. Heterogeneous phenotype in a

692 family with compound heterozygous parkin gene mutations. *Arch Neurol.* 2006;63(2):273-7.
693 35. Trempe J-F, Sauvé V, Grenier K, Seirafi M, Tang MY, Ménade M, et al. Structure of Parkin Reveals
694 Mechanisms for Ubiquitin Ligase Activation. *Science.* 2013;340(6139):1451-5.
695 36. Kumar A, Chaugule VK, Condos TEC, Barber KR, Johnson C, Toth R, et al. Parkin-
696 phosphoubiquitin complex reveals cryptic ubiquitin-binding site required for RBR ligase activity.
697 *Nature structural & molecular biology.* 2017;24(5):475-83.
698 37. Safadi SS, and Shaw GS. A disease state mutation unfolds the parkin ubiquitin-like domain.
699 *Biochemistry.* 2007;46(49):14162-9.
700 38. Spratt DE, Martinez-Torres RJ, Noh YJ, Mercier P, Manczyk N, Barber KR, et al. A molecular
701 explanation for the recessive nature of parkin-linked Parkinson's disease. *Nature*
702 *communications.* 2013;4:1983.
703 39. Tang MY, Vranas M, Krahn AI, Pundlik S, Trempe JF, and Fon EA. Structure-guided mutagenesis
704 reveals a hierarchical mechanism of Parkin activation. *Nature communications.* 2017;8:14697.
705 40. Okatsu K, Koyano F, Kimura M, Kosako H, Saeki Y, Tanaka K, et al. Phosphorylated ubiquitin
706 chain is the genuine Parkin receptor. *The Journal of cell biology.* 2015;209(1):111-28.
707 41. Kitada T, Asakawa S, Hattori N, Matsumine H, Yamamura Y, Minoshima S, et al. Mutations in
708 the parkin gene cause autosomal recessive juvenile parkinsonism. *Nature.*
709 1998;392(6676):605-8.
710 42. Grenier K, McLelland GL, and Fon EA. Parkin- and PINK1-Dependent Mitophagy in Neurons:
711 Will the Real Pathway Please Stand Up? *Frontiers in neurology.* 2013;4:100.
712 43. Whitworth AJ, and Pallanck LJ. PINK1/Parkin mitophagy and neurodegeneration—what do we
713 really know in vivo? *Current opinion in genetics & development.* 2017;44:47-53.

714

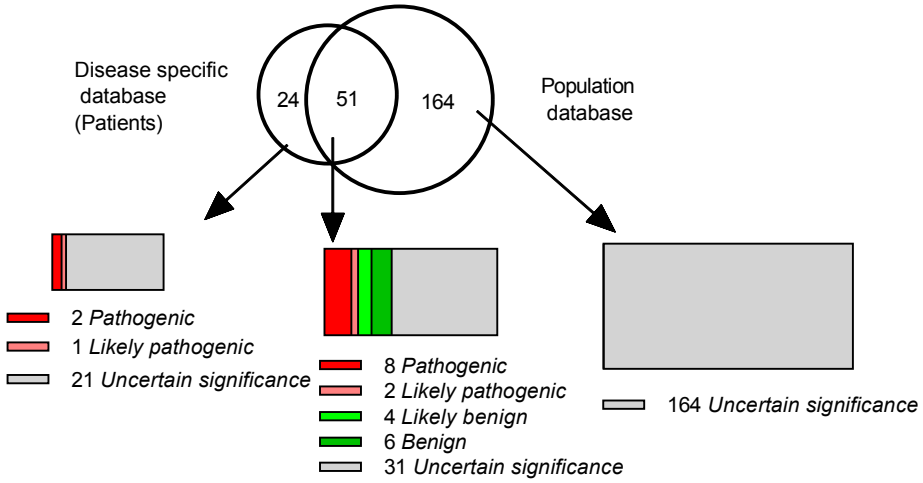

Figure 1. Clinical evidence is insufficient to determine pathogenicity of most *Parkin* missense variants. 75 *Parkin* missense variants were reported in disease specific databases (PDmutDB, MDSgene), 215 were reported in population databases (ExAC, dbSNP) and 51 were reported in both. Pathogenic and benign points were attributed for clinical evidence to each variant (Supplementary figure 1), which was then assigned with 1 of 5 standard terminologies using Sherloc (Supplementary figure 2): *Pathogenic* (red), *likely pathogenic* (pink), *likely benign* (green), *benign* (olive) and *uncertain significance* (grey).

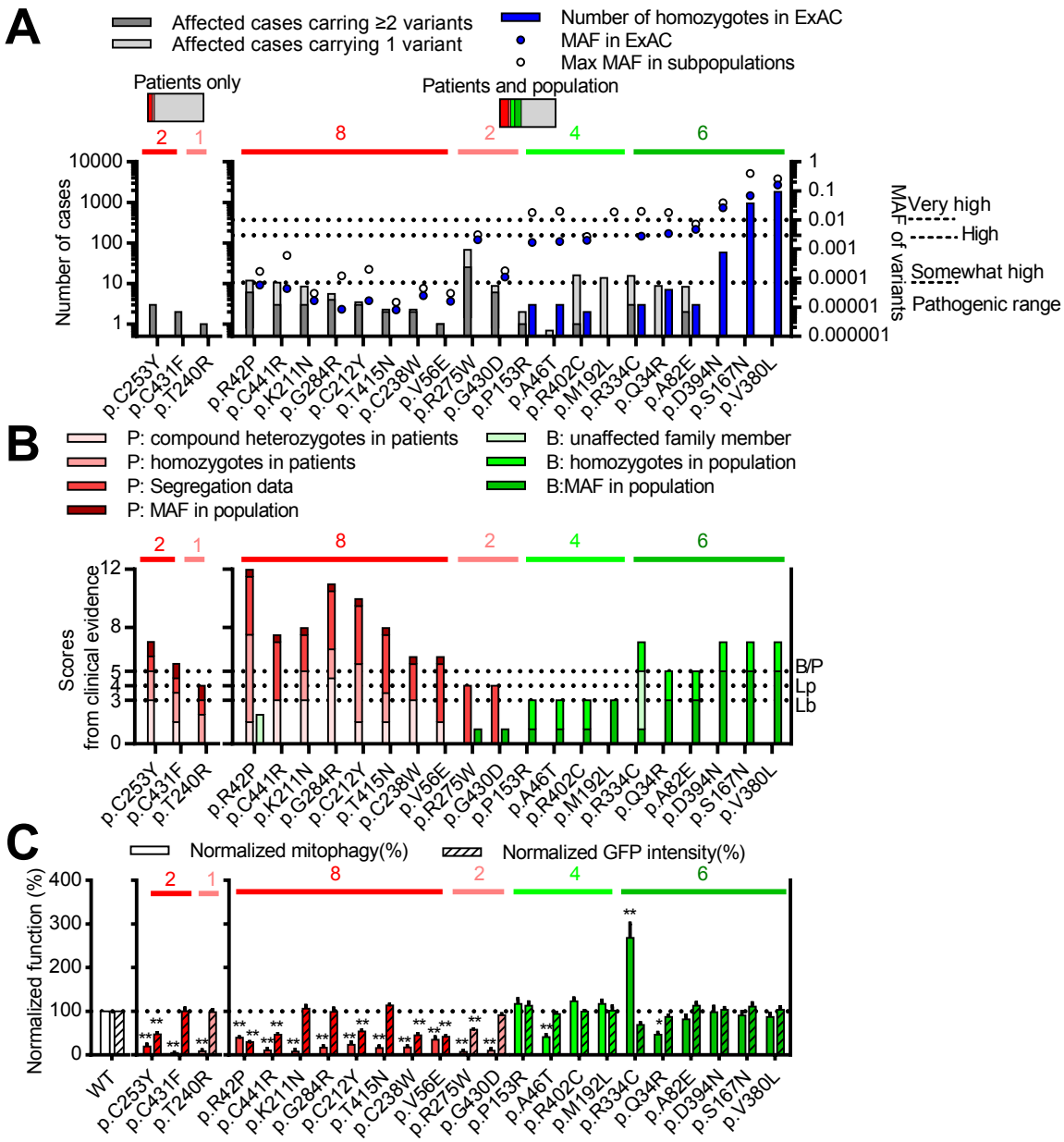

Figure 2. Most *Parkin* variants that could be clearly classified clinically displayed congruent functional profiles in cells. (A) Horizontal colored lines and numbers illustrate the classification of *Parkin* variants - *pathogenic* (red), *likely pathogenic* (pink), *likely benign* (green) and *benign* (olive) - and the number of variants in each category. For each variant, the number of cases (families or unrelated individuals) with PD carrying one or more than two *Parkin* variants were stacked and plotted in grey on the left Y axis. The number of homozygous individuals in ExAC was plotted in blue on the left Y axis. The minor allele frequency (MAF) in ExAC and maximum MAF in the subpopulations in ExAC and other population databases were plotted as blue and grey circles, respectively, on the right Y axis. Demarcations of MAF ranges are indicated by dotted lines. **(B)** For each variant, benign and pathogenic points from each line of clinical evidence were separately stacked. The dotted lines indicate thresholds for classification as *likely benign (Lb)*, *likely pathogenic (Lp)*, *benign (B)* or *pathogenic (P)*, based on Sherloc (Supplementary figure 2). **(C)** Quantification of the function of Parkin missense variants normalized to wildtype Parkin. Solid bars show mitophagy with 4h of CCCP treatment quantified from mtKeima signal in cells expressing GFP-Parkin variants. Hatched bars show GFP intensity of cells expressing GFP-Parkin variants. The colors of the bars represent the classification of the variants. * P<0.05, ** P<0.01, in one-way ANOVA with Dunnett's post-hoc test comparing the function of each variant with WT. N=3-7.

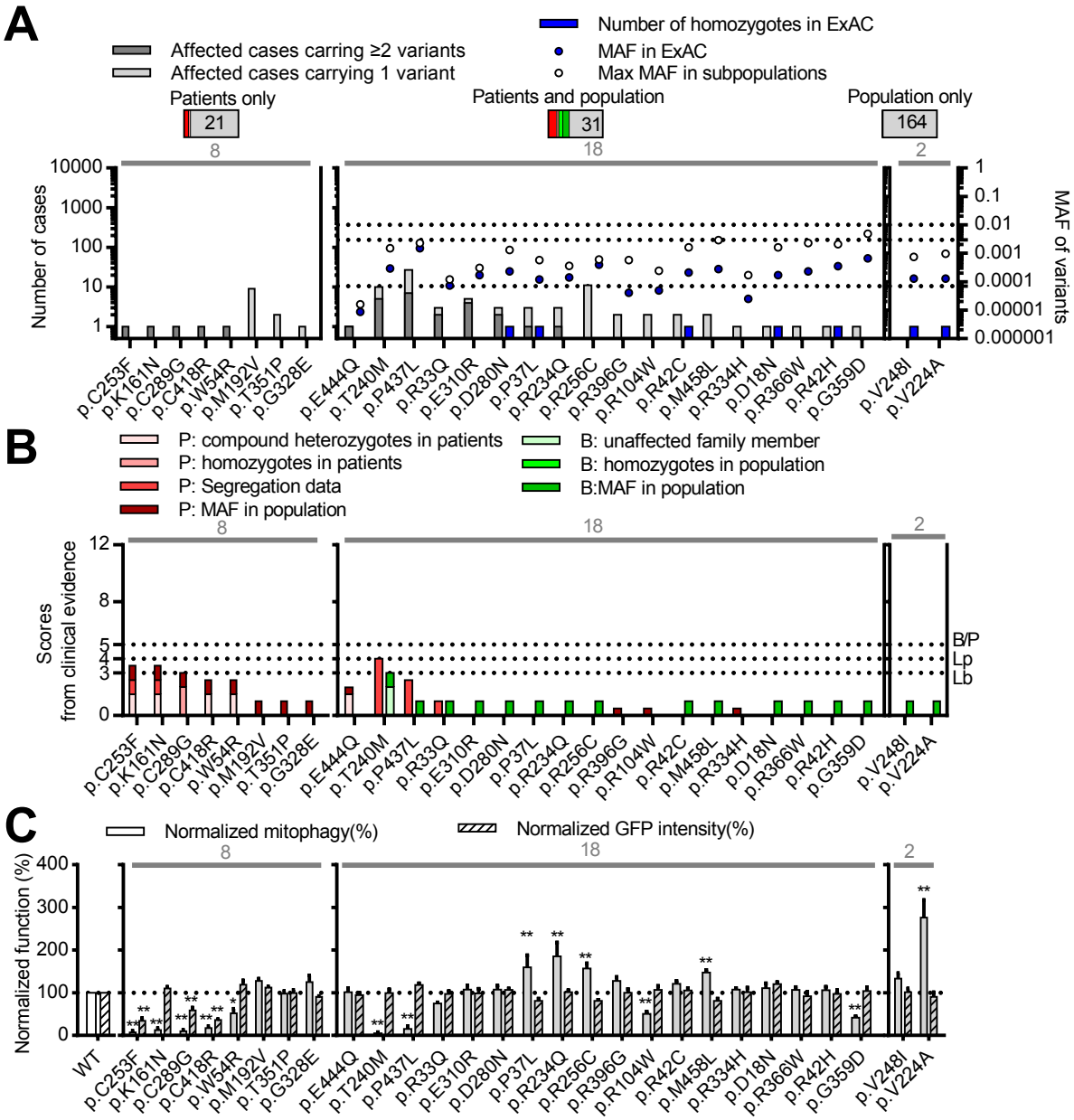

Figure 3. Most Parkin variants of *uncertain significance* based on clinical evidence displayed WT functional profiles in cells. (A) Data represented as in figure 2A. The grey lines and numbers represent *Parkin* variants classified as of *uncertain significance*. **(B)** For each variant, benign and pathogenic points from each line of clinical evidence were separately stacked. The dotted lines indicate thresholds as described in figure 2B. **(C)** Quantification of the function of Parkin missense variants in cells normalized to WT Parkin. Data represented as in figure 2C.

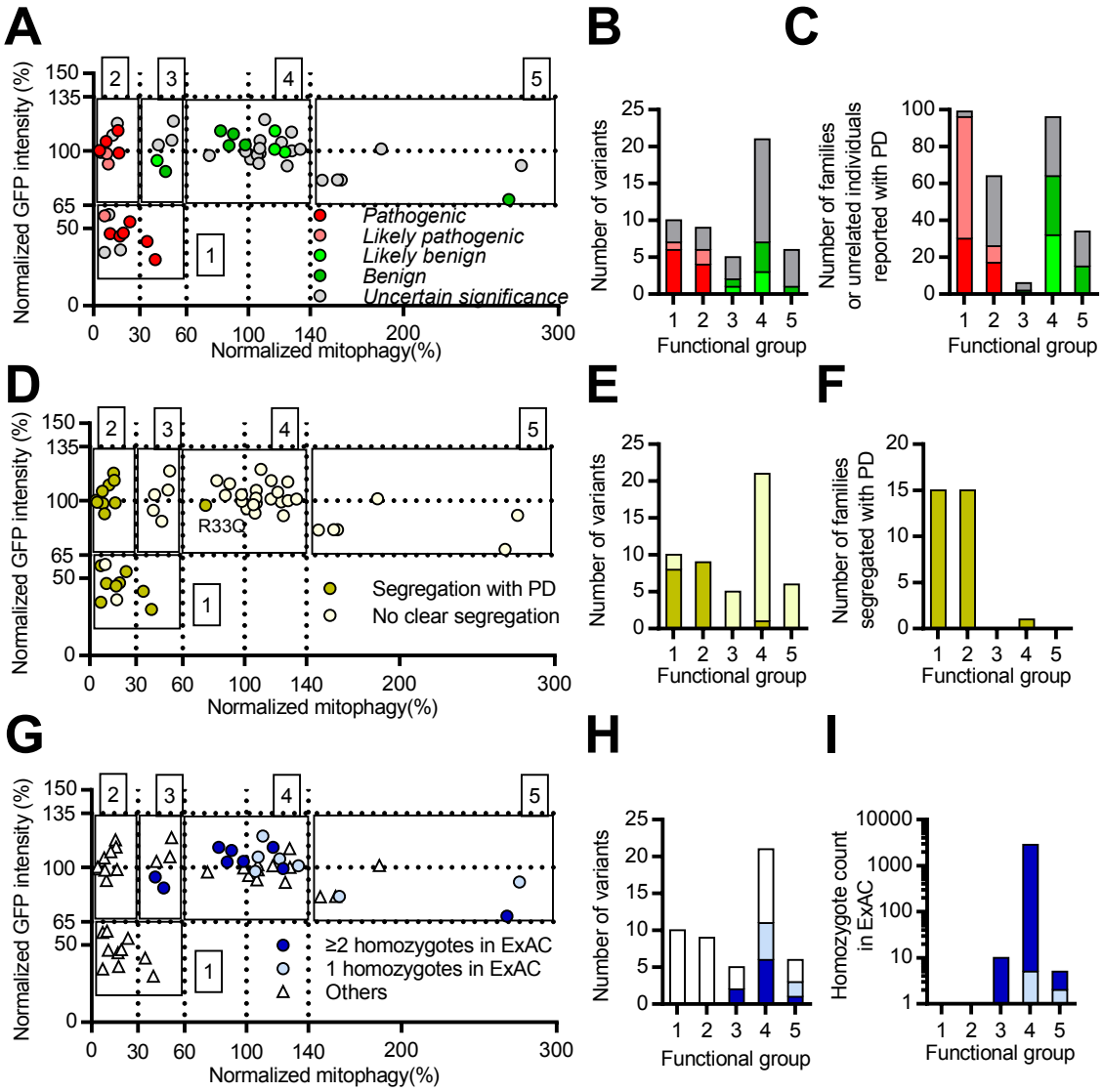

Figure 4. Parkin variants can be classified functionally in cells. (A) Functional alteration of variants assigned as *benign* (olive), *likely benign* (green), *pathogenic* (red), *likely pathogenic* (pink) and of *uncertain significance* (grey) based on clinical evidence were plotted for mitophagy activity on the X axis and GFP intensity on the Y axis. Functional alteration segregated into five groups, indicated by black boxes. 1. Significantly decreased mitophagy activity and GFP intensity compared with WT. 2. Severely decreased mitophagy activity with WT GFP intensity. 3. Moderately decreased mitophagy activity with WT GFP intensity. 4. WT mitophagy activity and GFP intensity. 5. Significantly increased mitophagy activity with WT GFP intensity. Distribution of the variants **(B)** and of the number of families or individuals carrying the variants **(C)** within each of the functional groups from (A). **(D)** Distribution of variants into the functional groups described in (A) according to their segregation (mustard) or lack of segregation (light-yellow) with PD in families. Quantification of the variants **(E)** and of the number of families in which the variants segregated with disease **(F)** per functional group. **(G)** The functional alteration of variants with more than 1 homozygote (blue), 1 homozygote (light-blue), or no homozygotes (white) in ExAC were plotted as in (A). Quantification of the variants **(H)** and of the number of homozygous individuals carrying the variants **(I)** per functional group.

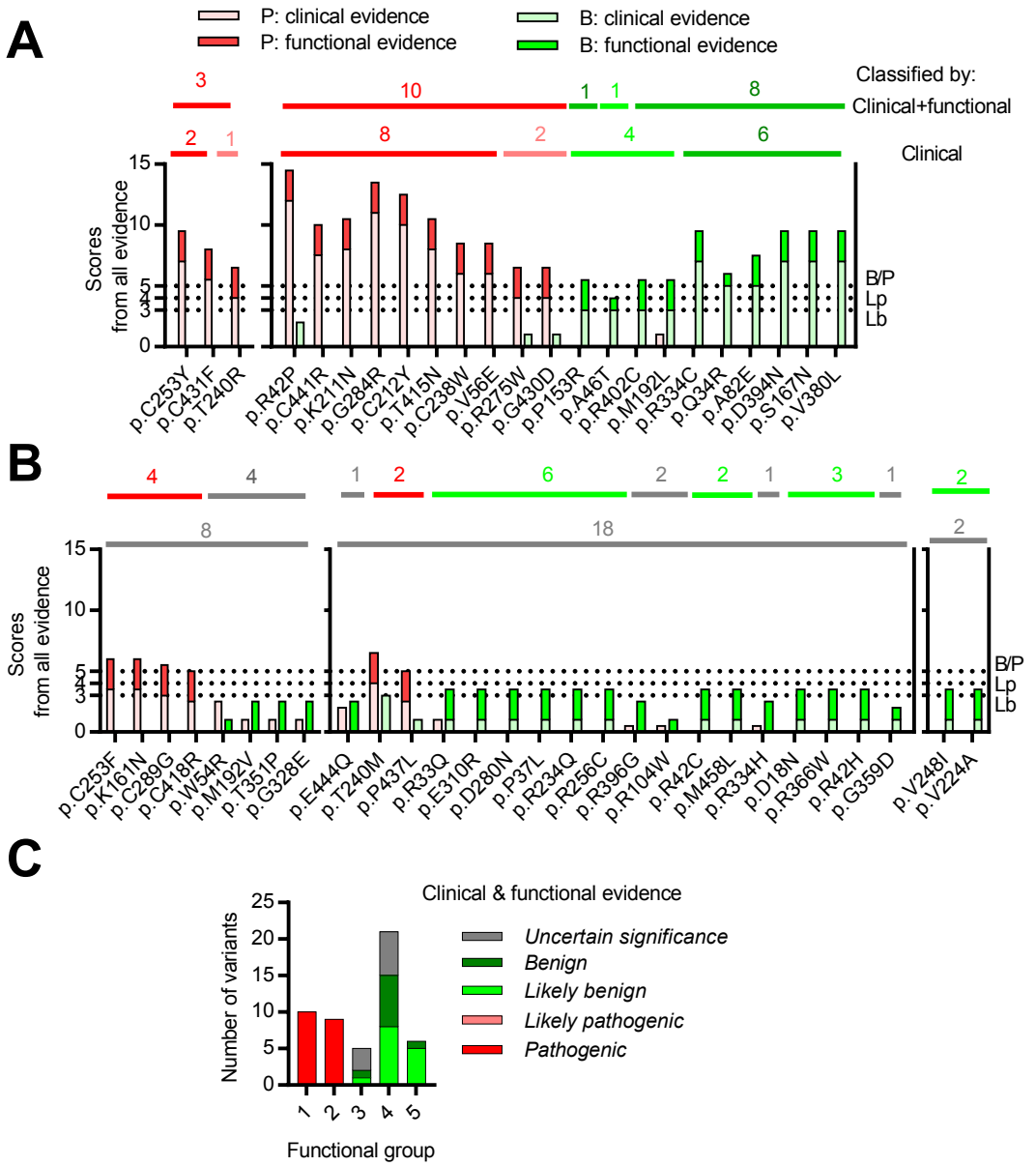

Figure 5. Integration of clinical and functional evidence refines the classification of *Parkin* variants. For each variant from figure 2 **(A)** and from figure 3 **(B)**, benign and pathogenic points from functional and clinical evidence were stacked and plotted separately. The dotted lines indicate thresholds for classification as *likely benign* (3B), *likely pathogenic* (4P), *benign* (5B) or *pathogenic* (5P). Horizontal colored lines and numbers represent the classification of the variants, *pathogenic* (red), *likely pathogenic* (pink), *likely benign* (green), *benign* (olive), and *uncertain significance* (grey), based on clinical or on clinical + functional evidence, and the number of variants in each category. Combining clinical and functional reduces the number of variants of *uncertain significance*. **(C)** Missense variants that impair Parkin function (functional groups 1 and 2 from figure 4) were all reclassified as *pathogenic*. In contrast, most variants that didn't severely impair Parkin function (group 3-5 from figure 4) were reclassified as *benign* or *likely benign*.

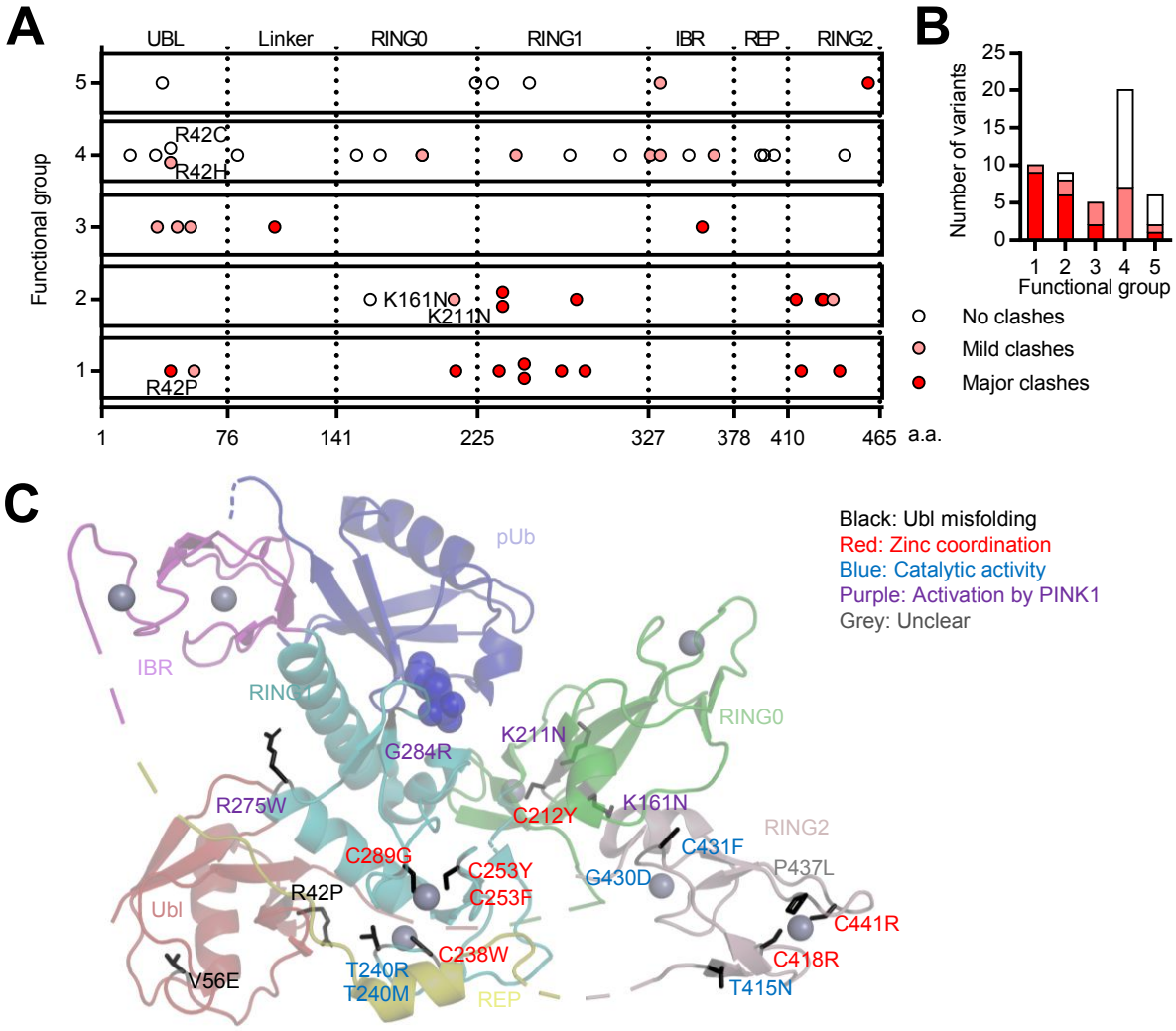

Figure 6. Structural analysis of *Parkin* variants reveals various pathogenic mechanisms. **(A)** Schematic representation of Parkin missense variants on Parkin protein 2D structure. Each circle indicates a missense variant. The location of the variant on the 2D sequence was plotted in the X axis with dotted lines separating the Parkin domains. The functional groups described in figure 4A, were plotted on the Y axis. The colors indicate the type of clash introduced by the missense variant. **(B)** Distribution of the variants from (A) within functional groups according to the type of clash they introduce. **(C)** Variants introducing functional alterations from group 1 and 2 were mapped onto the 3D structure of human Parkin bound to phospho-ubiquitin (PDB 5N2W). The side-chains of the amino acids substituted by the variants were highlighted in black. The blue spheres represent the phosphate of pUb. The grey spheres represent Zinc. The color of the text indicates the type of disruption to Parkin caused by the variant.

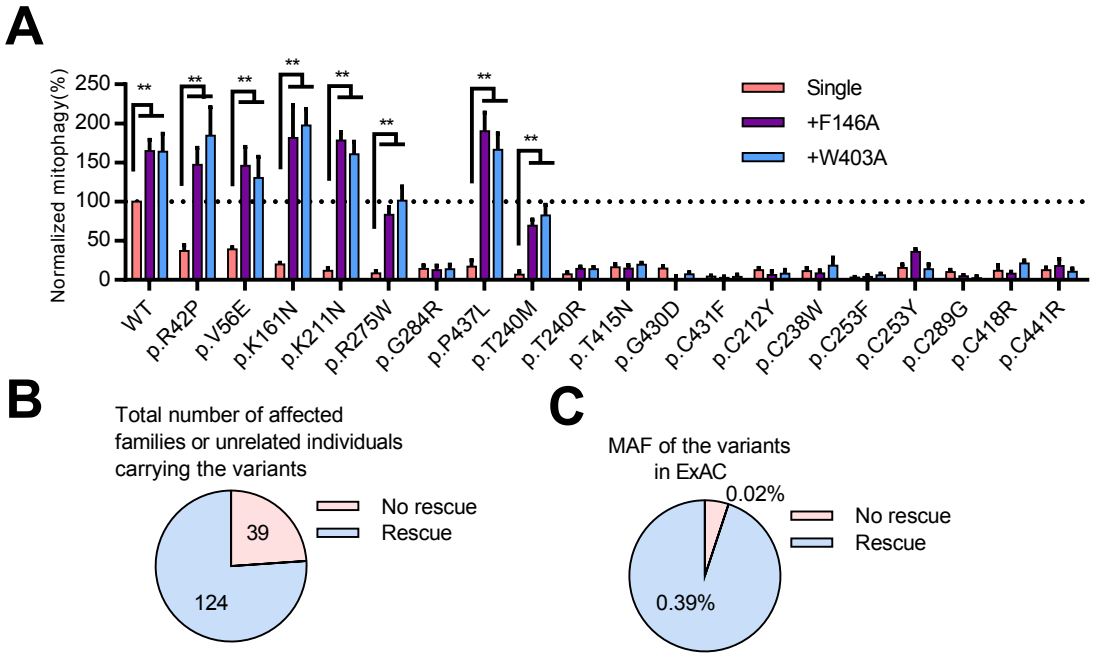

Figure 7. Structure-guided designer hyperactive Parkin mutants can rescue mitophagy in pathogenic variants. (A) Quantification of induced mitophagy after 4h of CCCP treatment in cells expressing WT GFP-Parkin, *pathogenic* missense variants, or W403A or F146A *in cis* with WT or *pathogenic* variants. Mitophagy mediated by each Parkin missense variant was normalized to that of WT Parkin in each repeat. * P<0.05, ** P<0.01, in two-way ANOVA with Dunnett's post-hoc test comparing the function of each variant with the variant *in cis* with W403A or F146A. N=3-7. **(B)** The number of families or individuals with PD carrying the *pathogenic* missense variants for which mitophagy was or was not rescued by the designer mutations are shown. **(C)** The MAF in ExAC of the *pathogenic* missense variants for which mitophagy was or was not rescued by the designer mutations are shown.

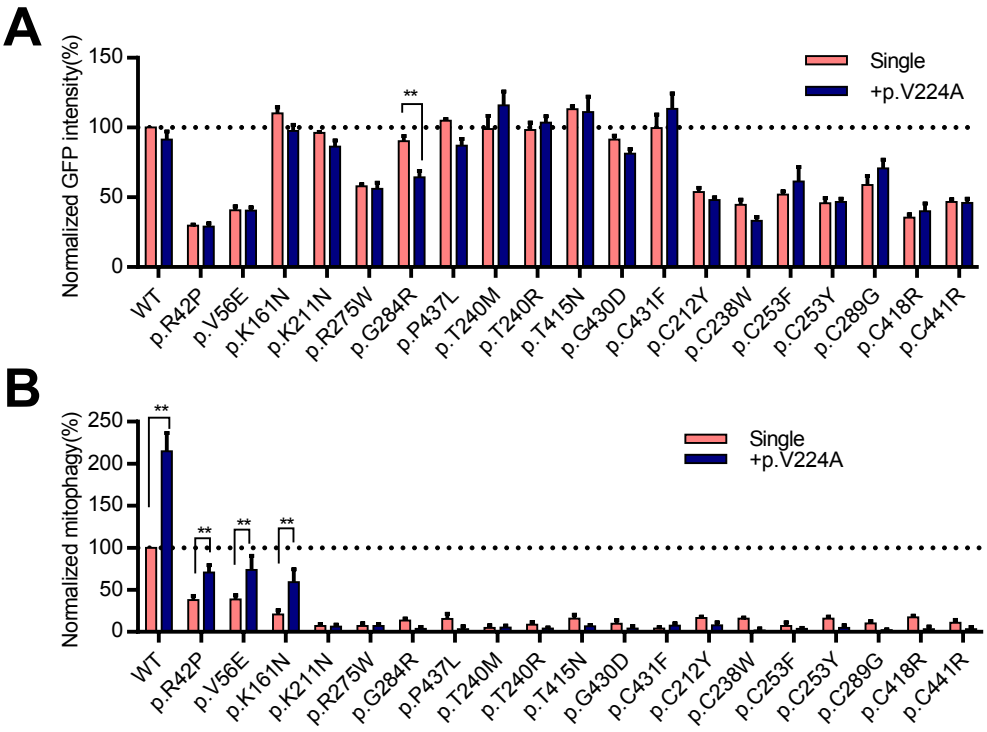

Figure 8. The naturally-occurring *Parkin* V224A hyperactive variant can rescue mitophagy in several *pathogenic* variants. (A) Quantification of GFP intensity from GFP signal by FACS in untreated cells expressing WT GFP-Parkin, *pathogenic* missense variants, or V224A *in cis* with WT or *pathogenic* variants. The GFP intensity for each Parkin missense variant was normalized to that for WT Parkin in each repeat. **(B)** Quantification of induced mitophagy with 4h of CCCP treatment in cells expressing WT GFP-Parkin, *pathogenic* missense variants, or V224A *in cis* with WT or *pathogenic* variants. Mitophagy mediated by each Parkin missense variant was normalized to that of WT Parkin in each repeat. * P<0.05; ** P<0.01, in two-way ANOVA with Dunnett's post-hoc test comparing the function of each variant with variant *in cis* with V224A. N=3-7 repeats.